

Composition Characterization of Methanesulfonic Acid

Daniel B. Roitman,^{†*} Jan McAlister, and Frank L. Oaks[‡]

Central Research & Development, Dow Chemical Company, 2800 Mitchell Drive, Walnut Creek, California 94598

Methanesulfonic acid (MSA) is often employed as a solvent for high-performance polymers such as poly(*p*-phenylene-*cis*-benzobisoxazole) or PBO, aramides, and conducting polymers. Since MSA is highly hygroscopic, and water has very strong effects on the physicochemical properties of the acid, it is important to develop methods to control and assess its composition. An approach involving the use of methanesulfonic anhydride (MSAA) is presented. The properties and compositions of MSAA solutions in MSA were investigated by combining ¹H NMR, conductimetry, viscometry, and differential refractometry. The results showed that previous studies involving MSA polymer solutions, and reported physical properties of MSA, were affected by water contamination. New values for the refractive index, viscosity, and specific conductivity of water-free MSA are presented.

Introduction

Methanesulfonic acid (MSA) is often employed as a solvent for lyotropic polymers such as poly(*p*-phenyleneterephthalamide) (PPTA) and poly(*p*-phenylene-*cis*-benzobisoxazole) (PBO). These polymers are not soluble in ordinary organic solvents and are usually characterized and processed in strong acid media (1-3) such as sulfuric acid (SA), poly(phosphoric acid) (PPA), methanesulfonic acid (MSA), and chlorosulfuric acid (CA). It is believed that these acids are capable of protonating one or several groups or atoms of each repeat unit of their stiff backbone (2), transforming the neutral polymers into polyelectrolytes. While the charge density of these polymers in solution is a subject of active research (4), it is well known that electrostatic interactions have strong effects on their solution behavior such as viscosity and light scattering (2, 3). A very serious problem encountered by researchers in this field, however, has been water absorption by the highly hygroscopic acids since water has dramatic effects on solubility, solution viscosity, and optical properties of the solutions. It is quite important, therefore, to develop methods to quantify their composition and to control water contamination.

The interest in nonaqueous acid solvents is not limited to polymers. In fact, strongly protonating solvents play very important roles in several areas of chemistry such as acid-catalyzed organic and inorganic reactions (5). The techniques described in this paper may be useful for researchers in those areas as well.

SA and stronger acids, like CA, were studied in great detail during the 1950s and 1960s primarily by Gillespie and co-workers (6-9). In those years there was considerable interest in acids stronger than SA, the so-called "superacids" (5). According to Bascombe and Bell (10), however, the Hammett acidity function H_0 of 100% MSA is only -7.86 compared with $H_0 = -11.3$ for SA (99.5 mass %). This might be the reason why MSA was not studied as thoroughly as its stronger counterparts.

While not as strong as SA, MSA is particularly useful as a solvent since it has a high boiling point, it does not generate corrosive fumes, it is less oxidizing than SA, it is relatively easy to dehydrate (see below), and it has a considerably lower ionic strength than SA. Some reported properties of this

Table 1. Physical Data Reported for Some Sulfonic Acids

solvent	$10^3 \kappa /$ (S-cm ⁻¹)	n_D^{20}	$\eta /$ (MPa-s)	$t_b / ^\circ\text{C}$	H_0	ϵ^a
SO ₃ H ₂ (SA) (6)	10.4	1.417	24.5	290-317	-11.3	101
ClSO ₃ H (CA) (8)	0.2-0.4	1.433	2.43	152-153	-12.78	60
CF ₃ SO ₃ H (CFA) (9)	0.22	1.331	2.81	161		

^a Dielectric constant.

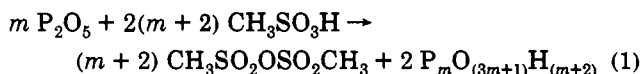
acid (11) (Table 1), such as the specific conductivity, however, appear to be incorrect because they were probably measured on water-contaminated samples, as will be shown in this paper.

In order to control MSA composition, we used methanesulfonic anhydride (MSAA). Several series of solutions containing MSAA/MSA were investigated, and the results were extrapolated to 100% MSA. Solutions containing MSA/H₂O were also investigated. Four different techniques, ¹H NMR, viscosity, conductimetry, and index of refraction, were utilized in this work to establish the properties of pure MSA.

Methods, Equipment, and Materials

To minimize water absorption, the work was carried out in a laboratory equipped with an air-dehydrating system which provided an environment between 4% and 8% relative air humidity at all times. Figure 1 illustrates the differences in water uptake rates by a droplet of acid under ordinary humidity conditions vs the "dry" laboratory. In addition, glassware was stored in a convection oven at ~120 °C to minimize water adsorption. Dried polymer samples and solutions were stored in nitrogen-blanketed plastic cases inside the low-humidity laboratory. These precautions efficiently prevented water contamination during sample preparation, handling, and storage.

MSA was purchased from both Fluka Chemika and Aldrich. The acid was distilled under vacuum in the presence of phosphorus pentoxide (P₂O₅) (12). The P₂O₅, which is one of the most hygroscopic compounds known, reacts with water to form poly(phosphoric acid) (PPA, bp > 300 °C). P₂O₅ is also capable of extracting water from MSA to form MSAA and PPA:



Three liters of methanesulfonic acid (Aldrich) and phosphorus pentoxide (300 g) was mixed in a 5-L-capacity round-bottom flask and heated to 70 °C for 3 h to complete the above

[†] Current address: Hewlett Packard Laboratories, 3500 Deer Creek Rd., Palo Alto, CA 94303.

[‡] Current address: Applied Biosystems, 850 Lincoln Center Dr., Foster City, CA 94404.

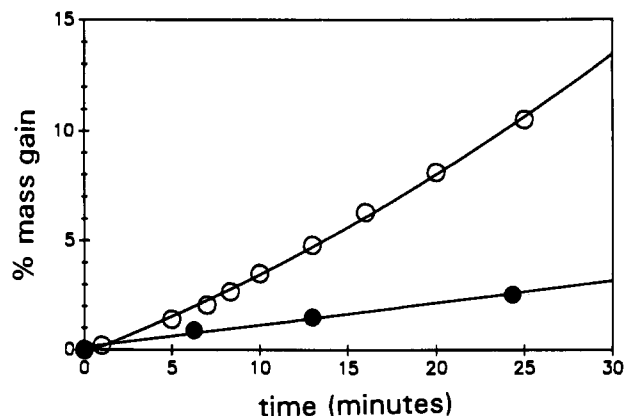


Figure 1. Rates of water absorption from air at 24 °C for MSA containing MSAA ($x_1 = 0.9$): open circles, 30% relative humidity; filled circles, 5% relative humidity. Three droplets (~ 0.07 g) were deposited on an open pan, and the mass gains were monitored.

reaction. The temperature of the mixture was raised to 90 °C, and the mixture was distilled through a 40-cm Vigreux column. A total of 3800 g was collected over a temperature range of 90–110 °C (at 0.3 mmHg) in 250-g fractions. The average collection rate was 5 mL/min. Teflon liners were used in all joints in order to avoid contamination. In order to minimize the formation of toxic decomposition products, the distillation flask was not heated beyond 112 °C.

The initial cuts of the distilled liquid solidified at ~ 70 °C. The white solid, MSAA, amounts to ~ 25 mass % of the total distillation product. The collecting head of the distillation apparatus was maintained hot during this stage to prevent solidification of MSAA. The next fraction of the distilled material ($\sim 15\%$) phase separated into a liquid and a solid, and the remaining distillation product (60%) was a clear colorless liquid at room temperature.

The compositions of the distilled cuts containing MSAA were determined by ^1H NMR. The MSAA peak has a higher chemical shift than MSA, as shown in Figure 2, and their proportions were determined from integration. We were unable to resolve the compositions of samples with excess water by NMR. Spectra were recorded on a QE-300 MHz spectrometer on neat samples. Sixteen scans were taken with a 10-s relaxation delay. T_1 relaxation times were measured for MSA and MSAA neat and dissolved in CD_2Cl_2 . The measured values of T_1 for MSA were 1.3 s (neat) and 0.59 s (in CD_2Cl_2). The measured values for MSAA were 1.7 and 0.55 s, respectively. The 10-s relaxation delay between scans is well above the time needed ($5T_1$) for complete relaxation.

Kinematic viscosities (ν) were measured using Ubbelohde capillary viscometers (Shott Gerate Type 501-20/II) in a thermostatic bath (Schott Gerate CT 1450) controlled to 25 ± 0.01 °C. The running times were usually in the range 70–110 s. The accuracy of the measurements was ± 0.03 s (less than 0.05% relative error).

Specific conductivities were measured using a YSI Model 35 conductimeter operating at 1 kHz. The cell was calibrated using water solutions of KCl. The measurements were carried out in the thermostatic bath used for viscometry. The accuracy of the conductivity was estimated to be $\pm 5 \times 10^{-6}$ S $\cdot\text{cm}^{-1}$. Refractive index increments were measured in a G. N. Woods differential refractometer (Newton, PA) equipped with two filters (632.8 and 546.1 nm). The cell was maintained at 25 ± 0.1 °C using a thermostatic bath, and the accuracy of the refractive index measurements was estimated to be better than $\pm 10^{-4}$.

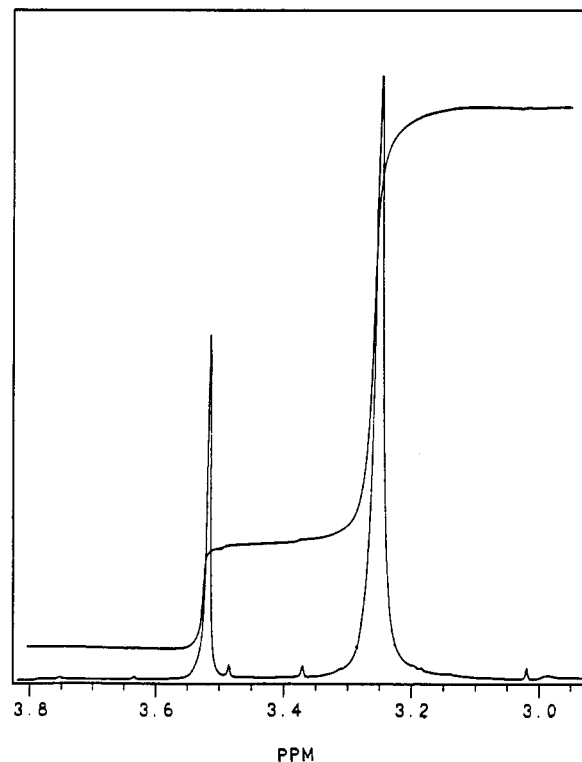


Figure 2. ^1H NMR (GE QE-300) of a MSA sample containing MSAA. The left peak corresponds to the MSAA hydrogens, the right one to the MSA ones. The side band corrected integration gives MSA composition $x_1 = 0.899$. Note that the integration over the MSA peak should be counted twice in order to account for the 2-fold difference in equivalent protons between MSAA and MSA. The sample showed $\nu = 9.2 \times 10^{-6}$ $\text{m}^2\cdot\text{s}^{-1}$. The least-squares regression, eq 5, estimates $\nu = 9.23 \times 10^{-6}$ $\text{m}^2\cdot\text{s}^{-1}$.

Table 2. Composition and Physical Characteristics of Distilled MSA in the Presence of 6 mass % P_2O_5

aliquot (cut)	$\nu / (10^{-6} \text{ m}^2\cdot\text{s}^{-1})$	$10^3 \kappa / (\text{S}\cdot\text{cm}^{-1})$	χ^2
A-E (750 mL)	solid		solid
F (250 mL)	mixed		biphasic
F1 (250 mL)	9.58	0.254	0.116
G (250 mL)	8.86	0.430	0.069
H (250 mL)	8.10	0.495	0.04
I (250 mL)	7.79	0.591	0.005
J (250 mL)	7.66	5.41	H_2O excess
K (250 mL)	7.99	15.25	H_2O excess
L (250 mL)	9.04	32.2	H_2O excess

Quantification of MSAA and Water in MSA

The distillation of MSA in the presence of P_2O_5 does not result in a liquid of uniform composition. Table 2 shows the viscosity and conductivity characteristics of the cuts of a typical distillation run. The composition of MSA, determined by NMR, is given by the mole fraction

$$x_i = n_i / (n_1 + n_2) \quad (2)$$

$$1 = x_1 + x_2 \quad (3)$$

where n_i is the number of moles of the i th species, and $i = 1$ corresponds to MSA and $i = 2$ corresponds to either MSAA or water, depending on which one is in excess (they do not coexist simultaneously in equilibrium).

Table 2 shows that the composition of the distilled liquid is not uniform. Furthermore, the table shows that distilling MSA from a mixture of MSA and P_2O_5 does not necessarily prevent water contamination from the latter part of the

Table 3. "Titration" of MSAA with Water Additions (25 °C)

sample	mass/g	n_1°	H ₂ O 10 ² n	$n_1^\circ + 2n$	10 ⁴ Δn (eq 6)	$\nu/(10^{-6} \text{ m}^2\text{s}^{-1})$	10 ³ $\kappa/(\text{S}\cdot\text{cm}^{-1})$	χ_2 (NMR)
1	stock	NA	0	NA	NA	9.108	0.334	0.092
2	52.548	0.4625	0.897	0.4804	-4	8.81	0.374	0.072
3	49.441	0.4351	1.80	0.4711	6.5	8.43	0.428	0.05
4	49.834	0.4386	1.93	0.4772	11.4	8.37	0.444	0.046
5	42.741	0.3761	2.96	0.4353	-1	7.91	0.534	0.021
6	48.591	0.4276	4.11	0.5098	3	7.65	0.569	0.005
7	47.054	0.4141	4.12	0.4965	3.8	7.60	0.585	0.002
8	37.691	0.3317	4.996	0.3989	163.5	7.62	5.7	0.039 w
9	29.339	0.2582	5.144	0.3105	252.8	8.42	22	0.075 w
10	29.548	0.2600	7.03	0.3127	439.8	8.76	26	0.123 w

distillation. Water is presumably generated by further condensation (chain extension) of PPA (13, 14). The kinematic viscosities of the aliquots decreased as the MSAA content decreased, reaching a minimum around $\nu = 7.6 \times 10^{-3} \text{ m}^2\text{s}^{-1}$, and then they increased again as the water content increased (cuts J-L). The corresponding specific conductivities, on the other hand, increased slowly with decreasing MSAA molar fraction, but increased rapidly for cuts J-L. The crossover point was near $\kappa \approx 0.59 \times 10^{-3} \text{ S}\cdot\text{cm}^{-1}$. The saturation of MSA with MSAA occurred approximately at $x_2 = 0.14$ at 25 °C.

In order to verify the accuracy of NMR for MSAA determination and to estimate the effects of water, we conducted a "titration" experiment assuming the following reaction:



where y of a stock solution was estimated using NMR, and n corresponds to controlled amounts of water added to the stock. The reactions were carried to completion for $n \leq y$ and for $n > y$.

The rates of reaction were found to be extremely slow at room temperature, and measurements were repeated over a 3-month period until stable values were reached.

A reference sample (stock) of composition $x_2 = 0.091$ MSAA (determined by NMR) was divided into 10 aliquots. Water was added to each aliquot to obtain a range of MSA/MSAA and MSA/H₂O compositions as shown in the last column of Table 3.

The kinematic viscosities and NMR-estimated molar fractions of MSAA of samples 1-7 in Table 3 were plotted on the right side of Figure 3 (circles). The data from the distillation cuts (F1-I) shown in Table 2 were also plotted (squares). The combined data from Tables 2 and 3 show an excellent linear correlation when $y > n$ (excess MSAA):

$$\nu/(10^{-6} \text{ m}^2\text{s}^{-1}) = 7.6 + 16.22x_2 \quad (5)$$

Therefore, the 100% MSA limiting kinematic viscosity is $\nu = 7.6 \times 10^{-6} \text{ m}^2\text{s}^{-1}$.

In order to establish the accuracy of the NMR technique, and to assess the degree of completion of eq 4, the theoretical compositions of each of the samples from 1 to 7 were compared to the compositions observed experimentally. Columns 2-4 of Table 3 show the initial number of moles of MSA in each sample (n_1°), the moles of water added, n , and the final number of MSA moles $n_1 = n_1^\circ + 2n$. The difference between the theoretical composition and the experimental one is given by

$$\Delta n = (n_1^\circ + 2n) - n_1^{\text{exp}} \quad (6)$$

where n_1^{exp} was estimated from the least-squares regression, eq 6, and the mole fraction relations, eqs 2 and 3. Column 5 of Table 3 shows that the agreement is indeed quantitative. In other words, NMR is capable of determining accurately the MSA/MSAA composition, and the reaction between water

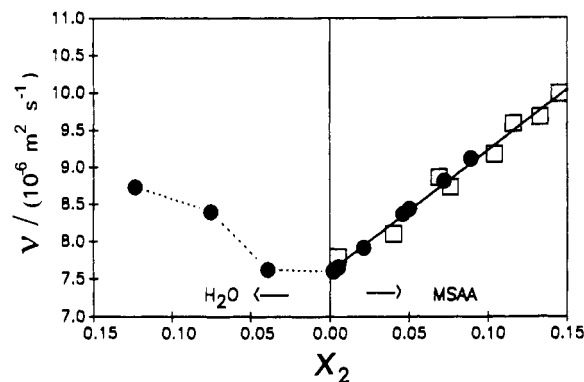


Figure 3. Dependence of MSA kinematic viscosity (ν) on molar fraction composition obtained by ¹H NMR. The right-hand side of the plot corresponds to solutions with excess MSAA, the left-hand side to solutions with excess water. The open squares correspond to distillation fractions, and the black circles identify the water "titration" experiment described in the text (Table 3). The highest point on the right corresponds to the solubility limit of MSAA at 25 °C ($x_2 = 0.14$). The kinematic viscosity of 100% MSA is $\nu = 7.6 \times 10^{-6} \text{ m}^2\text{s}^{-1}$, which corresponds to $\eta = 11.26 \text{ mPa}\cdot\text{s}$.

and MSAA, eq 4, is practically complete. The least-squares relation, eq 6, was used for the comparison in order to increase the accuracy, since we believe viscosity to be more precise than the NMR integration.

The compositions of samples numbered 8-10 in Table 3, on the other hand, were estimated directly stoichiometrically from eq 4, assuming the initial MSA/MSAA stock composition $x_1 = 1 - 0.092$. The viscosity of samples with excess water showed strongly nonlinear behavior (left-hand side of Figure 3). Notice that the viscosity of the acid actually increased with water content (water is 10-fold less viscous). This is an indication of strong interactions between the two components (14). Strong nonideal behavior is hardly surprising given the large exothermic process observed during dissolution of water in MSA. The minimum in the curve is achieved rather abruptly from the right (MSAA excess), but viscosity is not very sensitive to the water content and the results showed a shallow plateau to the left. Since there is a minimum in the viscosity-composition curve, viscosity cannot be used to define uniquely the composition of MSA. In addition to viscosity, Tables 2 and 3 also show specific conductivities of the samples. The combined data from Tables 2 and 3 are shown in Figure 4 (Figure 4b is a close-up view of the right-hand side of Figure 4a where MSAA is present). The conductivity of the samples containing MSAA decreased monotonically with MSAA content, following the linear relationship

$$\kappa/(10^{-3} \text{ S}\cdot\text{cm}^{-1}) = 0.586 - 2.92x_2 \quad (7)$$

The pure MSA extrapolation value at 25 °C corresponds to $0.59 \times 10^{-3} \text{ S}\cdot\text{cm}^{-1}$. The samples containing water [$n > y$ in eq 4] showed a dramatic nonlinear conductance increase with increasing water content. Conductivity, therefore, is a single-

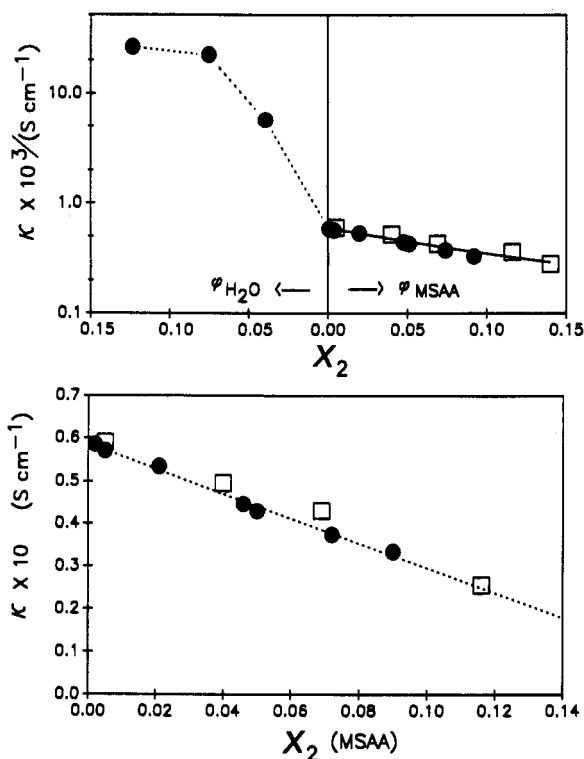


Figure 4. (a, top) Specific conductance of MSA (log scale) as a function of composition. The plot is divided as in Figure 3. Notice the dramatic, nonlinear increase of conductance caused by the presence of hydronium ions. (b, bottom) Linear relationship between the conductance and molar fraction of MSA. This is an expanded view of the right-hand side of Figure 4a. The open squares correspond to the distillation aliquots F1, G, H, and I listed in Table 2. The closed circles correspond to samples 1–7 in Table 3. The pure MSA least-squares extrapolation is $\kappa = 0.59 \times 10^{-3} \text{ S cm}^{-1}$. The linear decrease of ionic conductivity suggests that MSA is a neutral solute in MSA.

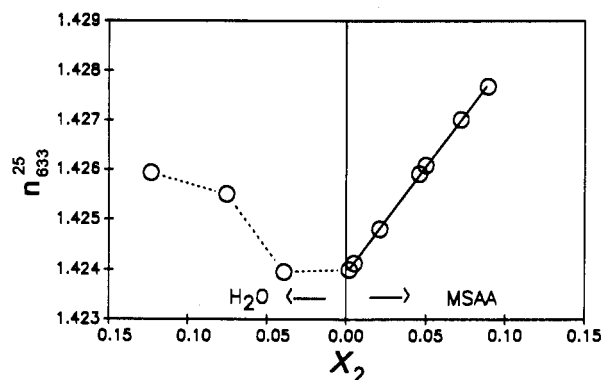


Figure 5. Refractive index dependence on MSA composition at $\lambda = 632.8 \text{ nm}$ (HeNe laser). The linear regression of samples with excess MSA extrapolates to $n_{633}^{25}(\text{MSA}) = 1.466$ and $n_{633}^{25}(\text{MSAA}) = 1.424$. The nonlinear refractive index increase of MSA with excess water suggests that the latter has strong effects on the structure of the liquid.

valued function of composition and very strong function of the water content.

The refractive index of the solutions was also investigated. Optical properties are very important for the light scattering study of polymers in these solvents. The refractive index of MSA changes with both MSA and water concentrations. Figure 5 shows the behavior for $\lambda = 632.8 \text{ nm}$, the wavelength of the HeNe laser, at 25°C . The right-hand side of the plot

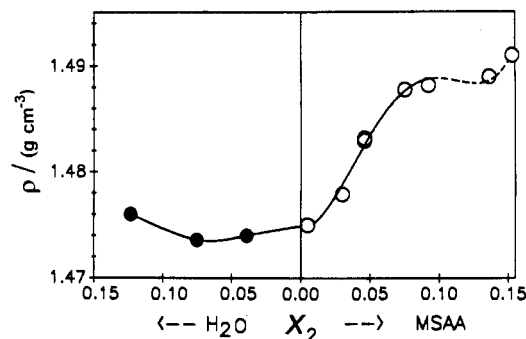


Figure 6. Density dependence on composition. The curves correspond to polynomial least-squares regressions given by eqs 9 and 10. The right-hand line probably exaggerates the curvature of the data trend at high MSA concentrations (broken segment). The highest point corresponds to MSA saturated at room temperature with MSA ($x_{\text{MSAA}} \approx 0.15$).

Table 4. Physical Data of 100% Methanesulfonic Acid (25°C)

ref	$10^8 \kappa / (\text{S cm}^{-1})$	n_D^{20}, n_{633}^{25}	$\eta / (\text{mPa s})$	$t_b / ^\circ\text{C}$
11	3–4	1.432	11.7	167
this work	0.59	1.430, 1.424	11.21	NA

can be fitted to the linear regression

$$n_{633}^{25} = 1.4239 + 0.042624x_2 \quad (8)$$

The intercept $n_{633}(\text{MSA}) = 1.4239 \pm 0.001$ was determined by differential refractometry interpolating the refractive indices of three standard compounds (1-octanol, $n = 1.424$; ethylene glycol, $n = 1.426$; and cyclohexane, $n = 1.421$). The indices of these compounds were reported at 435.8 and 546.1 nm at 25°C . The 632.8-nm corresponding values were determined by linear extrapolation. Using eq 8, the approximate refractive index of MSA ($x_2 = 1$) extrapolates to $n_{633}(\text{MSAA}) = 1.466$.

Finally, the density of the solutions was measured at 25°C with a Guy-Lussac-type specific gravity bottle (Ace Glass No. 5420). Figure 6 shows density vs composition. The curves shown correspond to the least-square polynomials

$$\rho / (\text{g cm}^{-3}) = 1.4747 - 0.01948x_2 + 7.6747x_2^2 - 90.755x_2^3 + 300.75x_2^4 \quad (9)$$

on the right side ($0 \leq x_{\text{MSAA}} \leq 0.15$) and

$$\rho / (\text{g cm}^{-3}) = 1.4749 + 0.01695x_2 - 0.3507x_2^2 - 4.549x_2^3 \quad (10)$$

on the left side ($0 \leq x_{\text{H}_2\text{O}} \leq 0.12$). The density of MSA ($x_1 = 1$) at 25°C is $\rho = 1.475 \text{ g cm}^{-3}$, and the density of MSA saturated with MSA ($x_{\text{MSAA}} = 0.15$) is $\rho = 1.491 \text{ g cm}^{-3}$.

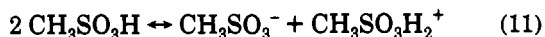
From $\nu = 7.6 \times 10^{-6} \text{ m}^2 \text{ s}^{-1}$ and $\rho = 1.475 \text{ g cm}^{-3}$, the viscosity of 100% MSA is given by $\eta = 11.21 \text{ mPa s}$ at 25°C .

Discussion

The above results clearly demonstrate that distilling MSA from a mixture of MSA and P_2O_5 results in fractions with a wide range of compositions: from MSA + MSA mixtures to fractions containing MSA + water. Since it is very unlikely that the water contamination of the latter fractions was introduced after the distillation, it is apparent that water was distilled jointly with the acid in these fractions.

The results also suggest that previously reported (11) physical properties of MSA were affected by water contamination. Table 4 compares these values with the results of this work. The most striking difference from previously reported values is the specific conductivity of water-free MSA.

Water is a strong base relative to MSA, and becomes protonated:



In order to establish the dissociation constant of eq 11, it would be necessary to know (or to estimate) the molar conductivities of the anion and cation. The transport of charged species in associating systems, such as water and sulfonic acids, is complex. It is currently accepted that charges are conducted via proton-transfer mechanisms (6). The unusually high conductivities and nonlinear behavior observed in samples containing water (Figure 4a, left side) are probably caused by a modification of the liquid structure of the acid caused by the hydronium ion (eq 12). This hypothesis is supported by the increase of the viscosity (15) and refractive index of MSA with water concentration. The investigation of mechanisms of ionic transport in associating liquids, however, lies outside the scope of this paper.

The physical behavior of samples containing MSAA, on the other hand, suggests that the anhydride is a neutral solute in MSA. The conductance of the liquid decreases linearly with MSAA contents, suggesting that the neutral molecules dilute the concentration of ions, the viscosity increases linearly as well, as expected from the addition of solute molecules larger than the solvent, and the index of refraction increases linearly. The solution density, on the other hand, appears to increase linearly with MSAA concentration, but the trend tapers off at higher concentrations. The acid becomes saturated at $x_{\text{MSAA}} \approx 0.15$ (25 °C).

Previously reported MSA viscosities are $\eta = 10.5$ mPa·s (11) and $\eta = 11.7$ mPa·s (16). Figure 4 suggests a ν minimum ($7.6 \times 10^{-6} \text{ m}^2\text{-s}^{-1}$) at the pure MSA composition which results in $\eta = 11.21$ mPa·s (since $\rho = 1.475 \text{ g}\cdot\text{cm}^{-3}$). It appears that the value reported in ref 11 is incorrect, and the one reported in ref 16 probably corresponds to a sample with water excess.

Summary

This work shows that it is not feasible to attain water-free MSA by simple distillation of commercial acid unless a stronger dehydrating agent, such as P_2O_5 , is added to the distillation vat. The composition of the distilled acid is not uniform, however, varying from MSAA rich in the earlier

stages of the distillation to water rich in the latter part. Water probably originates from PPA chain extension.

Several techniques were utilized to assess the mole fractions of MSA and MSAA, or MSA and water: NMR, conductivity, viscometry, and differential refractometry. The results showed that previously reported properties of MSA (specific conductivity, refractive index, viscosity) were very likely measured on water-contained samples.

To prepare samples of uniform MSA compositions, such as water-free MSA, it is necessary to add controlled amounts of MSAA and/or water to well-characterized stock solutions. The resulting solutions may require long times (from several days to months) to equilibrate, since the hydrolysis of MSAA is very slow at room temperature, especially in the neighborhood of 100% MSA.

The low specific conductivity of MSA free of water compared to sulfuric acid suggests that the dissociation constant of MSA is probably smaller by approximately 1 order of magnitude than it was previously assumed.

Acknowledgment

The authors would like to thank Dr. Ritchie Wessling and Dr. Charles Hotz for useful discussions and suggestions.

Literature Cited

- (1) Wolfe, J. F.; Sybert, P. D.; Sybert, J. R. U.S. Patent 4 533 692, 1985.
- (2) Wong, C. P.; Ohnuma, H.; Berry, G. C. *J. Polym. Sci., Polym. Symp.* 1978, 65, 173.
- (3) Metzger Cotts, P. C.; Berry, G. C. *J. Polym. Sci., Polym. Phys. Ed.* 1983, 21, 1255.
- (4) Roitman, D. B.; McAlister, J.; Martin, E.; Wessling, R. A. Submitted for publication in *J. Polym. Sci., Polym. Phys. Ed.*
- (5) Olah, G. A.; Suria Prakash, G. K.; Sommer, J. *Superacids*; John Wiley & Sons: New York, 1985.
- (6) Gillespie, R. J.; Robinson, E. A. In *Non-Aqueous Solvent Systems*; Waddington, T. C., Ed.; Academic Press: London and New York, 1965; Chapter 4.
- (7) Barr, J.; Gillespie, R. J.; Thompson, R. C. *Inorg. Chem.* 1964, 3, 1149.
- (8) Robinson, E. A.; Ciruna, J. A. *Can. J. Chem.* 1968, 46, 1719.
- (9) Haszeldine, R. N.; Kidd, J. M. *J. Chem. Soc.* 1954, 4228.
- (10) Bascombe, K. N.; Bell, R. P. *J. Chem. Soc.* 1959, 1096.
- (11) Paul, R. C.; Paul, K. K.; Malhotra, K. C. *J. Chem. Soc. A* 1970, 2712.
- (12) Field, L. *J. Am. Chem. Soc.* 1952, 74, 394.
- (13) Monsanto Phosphoric Acid. Technical Bulletin IC/DP-239R.
- (14) Fontana, B. J. *J. Am. Chem. Soc.* 1951, 73, 3348.
- (15) Irany, P. E. *J. Am. Chem. Soc.* 1943, 65, 1392.
- (16) Kim, C. S.; Berry, G. C. *J. Rheol. (N.Y.)* 1990, 34, 1011.

Received for review March 4, 1993. Accepted August 9, 1993. •

• Abstract published in *Advance ACS Abstracts*, November 15, 1993.